Third-order optical nonlinearities of $Zn_{1-x}Mg_xO$ thin films

Naibo Chen (陈乃波)[1,2], Huizhen Wu (吴惠桢)[1], Tianning Xu (徐天宁)[1], Ping Yu (余 萍)[1], and Dongjiang Qiu (邱东江)[1]

[1] *Department of Physics, Zhejiang University, Hangzhou 310027*

[2] *Department of Science, Zhijiang College of Zhejiang University of Technology, Hangzhou 310024*

Received January 13, 2005

The $Zn_{1-x}Mg_xO$ thin films were deposited on sapphire substrates by reactive electron beam evaporation deposition (REBED). The X-ray diffraction (XRD) measurement demonstrates that these films undergo phase transition from hexagonal to cubic with increasing the Mg concentration. Absorption coefficients at 532 nm of the samples were obtained from the absorption spectra. Using optical Kerr effect, the third-order susceptibilities of the ternary films over a wide range of Mg concentrations were determined. The magnitude of $\chi^{(3)}$ of the ternary $Zn_{1-x}Mg_xO$ films is order of 10^{-11} esu at $\lambda = 532$ nm. The sample with phase mixture of both hexagonal and cubic structures shows the largest third-order susceptibility. The difference observed in the magnitude of $\chi^{(3)}$ of $Zn_{1-x}Mg_xO$ films is attributed to the different microstructures of the ternary films, such as crystalline phase separation and crystal grains that enhance stimulated scattering.

OCIS codes: 190.4400, 310.6860, 190.3270.

Materials with large optical nonlinearities have received increased attention in the past years because they are crucial for the development of components for all-optical signal processing, and have many potential applications in electro-optic and integrated optical devices, nonlinear optical switching devices and real-time coherent optical signal processors[1−3]. ZnO, as a representatively wide band gap semiconductor, triggers research interesting on optical nonlinear-response in recent years, owning to its higher gain coefficient of laser oscillation[4], and its higher optical damage threshold than those of many common nonlinear materials[5]. The reported optical nonlinearities of ZnO, including second harmonic generation[6], second-order susceptibility $\chi^{(2)}$[7], and the third-order susceptibility $\chi^{(3)}$[8], render ZnO-based materials to be a promising candidate for the nonlinear optical applications.

As a family of ZnO-related compound, ternary $Zn_{1-x}Mg_xO$ with wider band gap than ZnO was first synthesized in 1998[9]. With the research on this novel material evolved into an important subject for material science, many advantages of their properties have been under active investigation, such as wide tuning range of the band gap energies (3.3—7.7 eV)[8−10] easily changed refractive index with the variation of Mg content[11], and ability to undergo phase evolution from hexagonal structure (Wurtzite) to cubic structure (NaCl-type) with the increase of Mg fraction in the ternary alloys[12]. It has suggested that the synthesis of $Zn_{1-x}Mg_xO$ would have provided a new way to tailor the optical and electronic properties. However, until now little investigation has been done on the nonlinear optical properties of this material, including third-order nonlinearities. Practically, most of the nonlinear optical devices should be concerned with the third-order optical susceptibility of materials. It is thus necessary to investigate the dependence of the optical nonlinearity of this material on the Mg concentration for their further application in nonlinear optical devices. In this paper, the third-order susceptibilities of $Zn_{1-x}Mg_xO$ films were determined using the technique of optical Kerr effect for the first time.

The $Zn_{1-x}Mg_xO$ ($x = 0 - 0.80$) thin films were grown on c-plane (0001) sapphire substrate by reactive electron beam evaporation deposition (REBED)[10]. High-purity (99.99%) ceramic targets of $(MgO)_y(ZnO)_{1-y}$ porcelain materials sintered at the temperature of 1250 °C were used as evaporation source. All samples were grown at a substrate temperature of 250 °C with an oxygen background pressure of 2×10^{-4} Torr. During the deposition, the working vapor pressure was kept constant of 3.5×10^{-4} Torr and the growth rate was about ~ 20 nm/min. The crystalline structures of the $Zn_{1-x}Mg_xO$ films were analyzed by X-ray diffraction (XRD) measurement. The Mg composition in ternary $Zn_{1-x}Mg_xO$ alloy films was determined by ultraviolet optical transmission measurements and theoretical procedure[10]. The transmission spectra of the $Zn_{1-x}Mg_xO$ films in the ultraviolet-visible region (190—900 nm) were measured by a Shimadzu UV-240 spectrophotometer with a light spot of 1.5×10 (mm) at room temperature.

The nonlinear optical properties of $Zn_{1-x}Mg_xO$ films were measured using time-resolved optical Kerr effect (OKE) technique. The configuration of the OKE experiments is shown in Fig. 1. The picosecond laser pulse

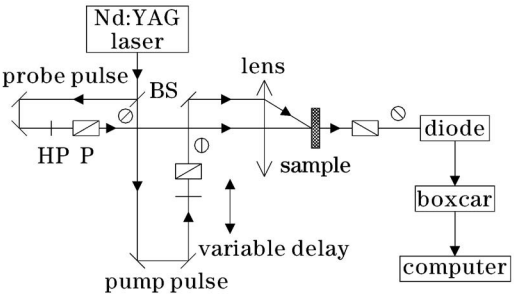

Fig. 1. The picosecond optical Kerr effect experiment apparatus arrangement. The circles and the lines show the polarization of the beams.

with full-width at half maximum (FWHM) of 30 ps and repetition rate of 10 Hz was generated from a mode-locked Nd:YAG laser system. A dichroic beam splitter was used to split the output pulse into two beams. One was used as a probe beam with the wavelength of 1064 nm (0.001-mJ pulse energy), and the other was used as a pump beam with the wavelength of 532 nm (0.127-mJ pulse energy). A variable optical attenuation consisted of a ratable half-wave plane (HP) and a Glan-polarizing prism, which could change the polarization of laser. Then two beams were focused onto the same position of the sample with diameters of 920 μm for pump and 115 μm for probe via a convex lens (15-cm focal length). The pump beam passing through a variable optical delay line was blocked after the sample. But the probe beam was sent through an analyzer with its transmission axis perpendicular to the original polarization of the probe beam. The final OKE signal was detected by a diode and a boxcar average, and recorded by a personal computer.

Figure 2 shows the XRD patterns of the $Zn_{1-x}Mg_xO$ films ($x = 0.18$, mixture of 0.37 and 0.75, 0.55) with three different crystalline phase structures grown on (0001) sapphire substrate. As can be seen from the XRD curves, the sample A (curve (a)) only shows a single hexagonal-phase orientation with its c-axis normal to the sapphire surface. The measured (0002) diffraction angle of the $Zn_{0.82}Mg_{0.18}O$ film is at 34.6°. But for the sample B (curve (b)), the diffraction peaks with both of hexagonal and cubic crystalline structures are observed. The peak at 34.8° is the (0002) diffraction from hexagonal phase $Zn_{0.63}Mg_{0.37}O$, while the peak at 36.7° is the (111) diffraction from cubic phase $Zn_{0.25}$ $Mg_{0.75}O$. The phenomenon of two-phase mixture has been observed in other studies of $Zn_{1-x}Mg_xO$ films ($x = 0.33 - 0.36$)[13] as well. For the sample C (curve c), only a single cubic phase (111) diffraction peak is seen. The measured (111) diffraction angle of the cubic phase $Zn_{0.45}Mg_{0.55}O$ is at 36.7°. Our previous studies revealed that $Zn_{1-x}Mg_xO$ films have single hexagonal phase structure when $x \leq 0.33$, single cubic phase structure when $x \geq 0.47$, and the mixture of both hexagonal and cubic phases when $0.33 < x < 0.47$[10]. Moreover, surface morphology of the films is also important for optical applications, because scattering losses deriving from a rough surface will affect the actual nonlinear optical properties. Therefore, in order to preclude the effect of the surface morphology of the films, samples were analyzed by atomic force microscope (AFM). The maximum roughness of the films for the scanning area of 1×1 (μm) is smaller than 4 nm, and the root mean square (RMS) roughness is only 0.51 nm, which implies the good smoothness and uniformity of the films.

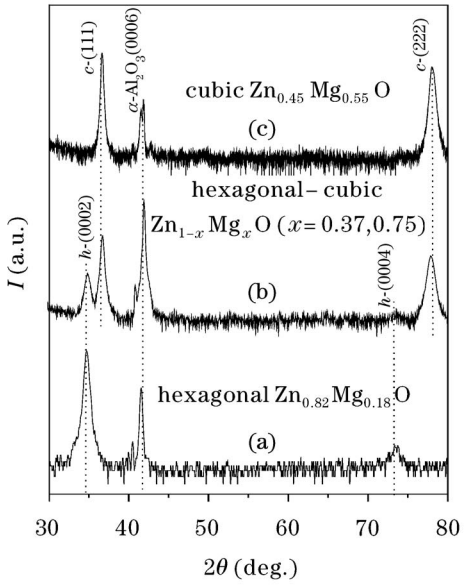

Fig. 2. XRD patterns of $Zn_{1-x}Mg_xO$ films ($x = 0.18$, 0.37, and 0.55).

Figure 3 shows three linear absorption spectra in the ultraviolet-visible region (180—900 nm) for three $Zn_{1-x}Mg_xO$ film samples. The absorption spectra were obtained by conversion of transmission spectra that are shown in the inset of Fig. 3. The absorption coefficient (α) of the $Zn_{1-x}Mg_xO$ alloy films was obtained from the measured transmission by $\alpha d = \ln(1/T)$, where d is the film thickness measured by an alpha-step profiler and T is the measured transmission. The absorption spectrum A is for the single cubic-phase $Zn_{0.20}Mg_{0.80}O$. The transmission spectrum for the cubic $Zn_{0.20}Mg_{0.80}O$ film in the inset shows a single absorption edge at ~200 nm (6.2 eV). The spectrum B is for the sample with mixture of hexagonal-phase $Zn_{0.63}Mg_{0.37}O$ and cubic-phase $Zn_{0.25}$ $Mg_{0.75}O$. Evidently, the transmission spectrum B in the inset demonstrates two absorption edges at ~ 305 and ~ 210 nm (4.1 and 5.9 eV), respectively. The absorption spectrum C is for the sample of single hexagonal-phase ZnO thin film. In the inset curve C displays one absorption edge at ~ 365 nm (~ 3.40 eV). The obvious shift of the absorption edge to shorter wavelength with the increase of Mg concentration is noticed. Based on the film thickness measured by an alpha-step profiler, the absorption coefficients at 532 nm for all samples are calculated, and the magnitudes of the absorption coefficients are comparable to those of ZnO and other II-VI semiconductors measured by other group.

As an example, the temporal evolution of the transient optical anisotropy of $Zn_{1-x}Mg_xO$ films with the single-phase and two-phase structures is shown in Fig. 4. It can be seen that the temporal behaviors of OKE signal of the samples are nearly symmetric with a peak centered

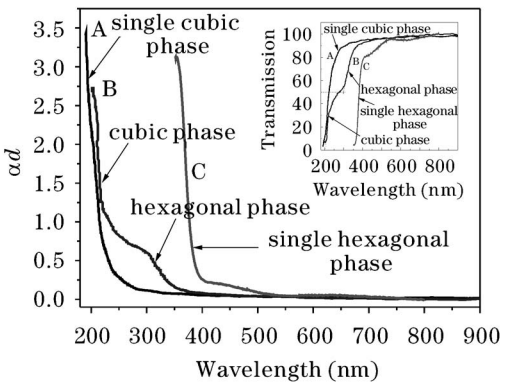

Fig. 3. Absorption spectra of single-phase $Zn_{0.45}Mg_{0.55}O$ and two-phase $Zn_{0.63}Mg_{0.37}O$ films measured at room temperature.

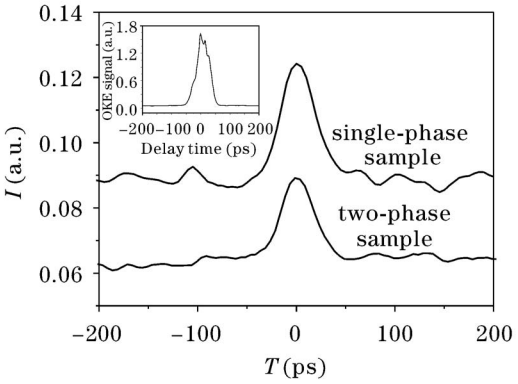

Fig. 4. The OKE response of single-phase $Zn_{0.45}Mg_{0.55}O$ and two-phase $Zn_{0.63}Mg_{0.37}O$ films. The OKE signal of water is shown in the inset for reference.

at zero delay point, and the FWHM (approximately 40 ps) of the band is comparable with the pulse duration. This ensures that the OKE response of the samples comes mainly from an instantaneous process corresponding to the electronic response, and the non-instantaneous processes should be ignored. Using the standard procedure of reference measurement, the magnitude of the third-order nonlinear susceptibility $\chi^{(3)}$ can be calculated from the OKE measurement by[14]

$$\chi_{\rm s}^{(3)} = \chi_{\rm r}^{(3)}(I_{\rm s}/I_{\rm r})^{1/2}(n_{\rm s}/n_{\rm r})^2(L_{\rm r}/L_{\rm s}) \times \alpha L_{\rm s}/R, \quad (1)$$

$$R = \exp(-\alpha L_{\rm s}/2)[1 - \exp(-\alpha L_{\rm s})], \quad (2)$$

where I is the intensity of the OKE signal at zero delay time, L is the interaction length of pump beam and probe beam over the sample and reference, n is the linear refractive index, α is the linear absorption coefficient of the samples, and subscript s and r represent the sample and reference, respectively. The linear refractive indices of our samples at 532 nm were determined from transmission measurements and Manifacier envelope method[16]. Water was used as the reference sample, and the values of $\chi_{\rm r}^{(3)}$, $L_{\rm r}$, and $n_{\rm r}$ are 2.80×10^{-14} esu[15], 0.5 cm, and 1.33, respectively. The ratio of the OKE intensity from the samples to that from water reference given in Eq. (1) was taken to eliminate the measurement errors caused by laser power fluctuations. Furthermore, the effect of $\chi^{(3)}$ of the substrate on the results was ignored because the absorption coefficient and the third-order susceptibility of sapphire are several orders smaller than the measured $Zn_{1-x}Mg_xO$ film samples. Based on Eqs. (1) and (2), the third-order nonlinear susceptibility of ZnO film (950-nm thickness) is also calculated. The value of 4.65×10^{-11} esu is comparable with that of 5.7×10^{-11} esu for ZnO thin films reported previously[17], which indicates the stability of the laser system and the reliability of the measurement results.

The sample parameters and the calculated third-order nonlinear susceptibility $\chi_{\rm s}^{(3)}$ values of $Zn_{1-x}Mg_xO$ films are given in Table 1. It is evident that the third-order optical nonlinearity of the $Zn_{1-x}Mg_xO$ ($x = 0.37$, 0.75) sample with mixture of two-phase structures is larger than those of $Zn_{1-x}Mg_xO$ samples with a single hexagonal- or cubic-phase structure. Compared with hexagonal $Zn_{1-x}Mg_xO$ films, cubic phase $Zn_{1-x}Mg_xO$ films have relatively small third-order susceptibilities and the value of $\chi^{(3)}$ decreases with the increase of Mg concentrations. Usually, several factors would affect the magnitude of $\chi^{(3)}$ of $Zn_{1-x}Mg_xO$ films. Among these factors, the phase transition of the films from hexagonal to cubic with the increase of Mg concentration could be believed to tightly correlate with the magnitudes of $\chi^{(3)}$ in $Zn_{1-x}Mg_xO$ films. We know that if the in-plane orientations of the unit cells for the films are different, the atomic bounds deviating from their equilibrium position will result in extra carriers, and the higher the carrier density is, the larger the optical nonlinearity should be. Also, the crystal grains emerged in the films will significantly increase the nonlinear fraction by enhancing stimulated scattering[5]. So the difference observed in the $\chi^{(3)}$ of $Zn_{1-x}Mg_xO$ films can be attributed to the different microstructures of the ternary films. In comparison to the single hexagonal- or cubic-phase $Zn_{1-x}Mg_xO$ films, $Zn_{1-x}Mg_xO$ ($x = 0.37$, 0.75) sample with mixture of two-phase structures is normally prone to generate a number of crystal grains because of the large mismatch between its hexagonal- and cubic-phase structures. It thus allows us to suppose that the larger nonlinear optical susceptibility of $Zn_{1-x}Mg_xO$ ($x = 0.37$, 0.75) film may arise mainly from its different in-plane orientations of the unit cells and strong scattering caused by the crystal grains. In addition, two-photon resonance may also contribute to nonlinear refraction in the samples of the hexagonal-phase and two-phase $Zn_{1-x}Mg_xO$ films because from the absorption spectrum shown in Fig. 3, the normalized incident photon energy of $\hbar\omega = 2.33$ eV ($\lambda = 532$ nm) is larger than $E_{\rm g}/2$ of the hexagonal-phase $Zn_{1-x}Mg_xO$, which does satisfy the two-photon absorption condition $1/2E_{\rm g} < \hbar\omega < E_{\rm g}$ [17].

In summary, the nonlinear optical response of $Zn_{1-x}Mg_xO$ films ($x = 0 - 0.80$) with three different structures was studied by using absorbance and OKE measurement techniques. The magnitude of third-order nonlinear susceptibility $\chi^{(3)}$ of the ternary $Zn_{1-x}Mg_xO$

Table 1. Parameters of $Mg_xZn_{1-x}O$ Films

Sample (Mg Fraction x)	$n_{\rm s}$ (Refraction Index)	$I_{\rm s}/I_{\rm r}$ (Ratio of OKE Signal)	$L_{\rm s}$ (μm) (Interaction Length)	$\chi^{(3)}$ ($\times 10^{-11}$ esu) (Third-Order Nonlinear Susceptibility)
0.00	1.91	0.0213	0.95	4.65
0.18	1.86	0.0147	0.60	5.70
0.37, 0.75	1.85	0.0176	0.47	7.80
0.55	1.84	0.0238	0.83	5.06
0.80	1.74	0.0343	1.25	3.64

films is order of 10^{-11} esu at $\lambda = 532$ nm. The largest nonlinear susceptibility was observed in $Zn_{1-x}Mg_xO$ ($x = 0.37, 0.75$) films that have the mixture of hexagonal- and cubic-phase structures. Together with the absorption characteristics, the difference observed in the magnitude of $\chi^{(3)}$ of $Zn_{1-x}Mg_xO$ films is attributed to the different microstructures of the ternary films, such as crystalline phase separation and crystal grains that enhance stimulated scattering.

The authors would like to acknowledge the measurement of time-resolved optical Kerr effect of the ternary $Zn_{1-x}Mg_xO$ films by Dr. X. Liu of the Department of Optical Science and Engineering in Fudan University. This work was supported by the National Natural Science Foundation of China under Grant No. 10174064 and 50472058. H. Wu is the author to whom the correspondence should be addressed, his e-mail address is hzwu@zju.edu.cn.

References

1. S. Priyadarshy, M. J. Therien, and D. N. Beratan, J. Am. Chem. Soc. **118,** 1504 (1996).
2. Y. Imanishi and S. Ishihara, Thin Solid Films **331,** 309 (1998).
3. H. M. Gibbs, G. Khitrova, and N. Peyghambarian, *Nonlinaear Photonics* (Springer, Berlin Heidelberg, New York, 1990).
4. Z. K. Tang, G. K. L. Wang, P. Yu, M. Kawasaki, A. Ohtomo, H. Koinuma, and Y. Segawa, Appl. Phys. Lett. **72,** 3270 (1998).
5. C. Y. Liu, B. P. Zhang, N. T. Binh, and Y. Segawa, Appl. Phys. B: Laser and Optics **79,** 83 (2004).
6. Z. K. Tang, G. K. L. Wang, P. Yu, M. Kawasaki, A. Ohtomo, H. Koinuma, and Y. Segawa, Appl. Phys. Lett. **70,** 2230 (1997).
7. H. Cao, J. Y. Wu, H. C. Ong, J. Y. Dai, and R. H. Chang, Appl. Phys. Lett. **73,** 572 (1998).
8. S. Choopun, R. D. Vispute, W. Yang, R. P. Sharma, T. Venkatesan, and H. Shen, Appl. Phys. Lett. **80,** 1529 (2002).
9. A. Ohtomo, M. Kawasaki, T. Koida, K. Masubuchi, H. Koinuma, Y. Sakurai, Y. Yoshida, T. Yasuda, and Y. Segawa, Appl. Phys. Lett. **72,** 2466 (1998).
10. N. B. Chen, H. Z. Wu, D. J. Qiu, T. N. Xu, J. Chen, and W. Z. Shen, J. Phys.: Condens. Matter **16,** 2793 (2004); J. Chen, W. Z. Shen, N. B. Chen, D. J. Qiu, and H. Z. Wu, J. Phys: Condens. Matter **15,** L475 (2003).
11. C. W. Teng, J. F. Muth, U. Ozgur, M. J. Bergmann, H. O. Everitt, A. K. Sharma, C. Jin, and J. Narayan, Appl. Phys. Lett. **76,** 979 (2000).
12. I. Takeuchi, W. Yang, K.-S. Chang, M. A. Aronova, T. Venkatesan, R. D. Vispute, and L. A. Bendersky, J. Appl. Phys. **94,** 7336 (2003).
13. A. K. Sharma, J. Narayan, J. F. Muth, C. W. Teng, C. Jin, A. Kvit, R. M. Kolbas, and O. W. Holland, Appl. Phys. Lett. **75,** 3327 (1999).
14. M. K. Casstevens, M. Samoc, J. Pfleger, and P. N. Prasad, J. Chem. Phys. **92,** 2019 (1990).
15. F. Kajzar and J. Messier, Phys. Rev. A **32,** 2352 (1985).
16. N. B. Chen, H. Z. Wu, and T. N. Xu, J. Appl. Phys. **97,** 023515 (2005).
17. R. Y. Wang, X. C. Wu, B. S. Zou, L. Wang, S. S. Xie, J. R. Xu, and W. Huang, Mat. Res. Innovat **2,** 49 (1998).